Thermochromic properties of the ferroelectric Cu^{2+}-doped $[(CH_3)_4N]HgBr_3$: study of the temperature-induced dichroism

1999 J. Phys.: Condens. Matter 11 2595

(http://iopscience.iop.org/0953-8984/11/12/014)

J. Phys.: Condens. Matter **11** (1999) 2595–2606. Printed in the UK PII: S0953-8984(99)99042-2

Thermochromic properties of the ferroelectric Cu^{2+}-doped $[(CH_3)_4N]HgBr_3$: study of the temperature-induced dichroism

Rafael Valiente and Fernando Rodríguez†

DCITIMAC, Facultad de Ciencias, Universidad de Cantabria, 39005 Santander, Spain

Received 3 November 1998

Abstract. A new thermochromic material formed by doping Cu^{2+} into the ferroelectric $(TMA)HgBr_3$ ($TMA = (CH_3)_4N$) crystal is presented. The change of colour from green (room temperature) to red (low temperature) under polarized light observation is accompanied by a strong temperature-induced dichroism at low temperature. The origin of these phenomena is investigated through the polarized charge transfer spectra associated with Cu^{2+} complexes formed in the title compound, and their dependence on temperature in the 10–300 K range. Attention is paid to correlating the optical spectra with the local structure around Cu^{2+}. The results are compared with those obtained in the tribromide $(TMA)Cd[Cu]Br_3$ and $(TMA)Mn[Cu]Br_3$, and the tetrabromide $(TMA)_2Hg[Cu]Br_4$ and $(TMA)_2Cd[Cu]Br_4$ crystals, where Cu^{2+} forms $CuBr_6^{4-}$ complexes of nearly D_{4h} symmetry, and tetrahedral distorted $CuBr_4^{2-}$ complexes of D_{2d} symmetry, respectively. An interesting feature is the presence of a strongly polarized absorption band at 15 800 cm^{-1} in $(TMA)Hg[Cu]Br_3$, which is responsible for the observed dichroism and thermochromism. The existence of this band is associated with the formation of highly distorted $CuBr_4^{2-}$ complexes in the monoclinic $(TMA)HgBr_3$ host crystal. The enhancement of dichroism exhibited by this crystal with decreasing temperature is noteworthy. The analysis of the spectra reveals that this unusual thermal behaviour can be explained in terms of thermally activated reorientations rather than structural changes of the Cu^{2+} complex.

1. Introduction

The optical properties such as colour or dichroism of copper halide compounds are in many cases due to Jahn–Teller (JT) distorted complexes CuX_4 or CuX_6 (X = Cl, Br) formed by Cu^{2+} and their ligands X. In chlorides like in oxides, the colour is governed by the optical window defined by the first ligand-to-metal $X^- \rightarrow Cu^{2+}$ charge transfer (CT) band placed at 26 000 cm^{-1}, and the high-energy crystal field (CF) band around 10 000–16 000 cm^{-1}, depending on the type of ligand and the degree of the JT distortion [1–5]. In particular, this optical window is defined by the energy, the intensity and the width of these two bands. For copper complexes, these spectroscopic parameters strongly depend on the local geometry around Cu^{2+} (symmetry and bond distances) and, therefore, structural transformations of the complex induced either by temperature or by pressure may induce significant changes of colour of the material (thermochromism or piezochromism, respectively), making copper systems attractive for using as *sensors*. The pure copper compounds $[(C_2H_5)_2NH_2]_2CuCl_4$ [6] and $(CH_3NH_3)_2CuCl_4$ [7] are examples of this behaviour.

In bromides, however, the colour is mainly determined by the intense $Br^- \rightarrow Cu^{2+}$ CT bands, since, at variance with chlorides, the CT spectra spread over the whole visible

† Author to whom correspondence should be addressed.

range due to the overall redshift of about 5000–10 000 cm^{-1} experienced by CT bands of copper complexes when Cl^- is replaced by Br^- [8, 9]. This redshift is in agreement with the 6000 cm^{-1} predicted from the optical electronegativity difference of these two ligands ($\Delta\chi = \chi(Cl^-) - \chi(Br^-) = 0.2$) [10]. In addition, copper bromide systems can exhibit a marked dichroism given that the electric-dipole allowed CT transitions are, in first approximation, completely polarized either along the JT distortion axis (z polarized) of the complex or in the perpendicular plane (x, y polarized). This aspect is noteworthy since it can be exploited in the search of optical materials, particularly, Cu^{2+}-doped anisotropic bromide systems, which can accommodate $CuBr_4^{2-}$ or $CuBr_6^{4-}$ units along preferential symmetry directions.

The aim of this paper is to investigate the optical properties of the ferroelectric (TMA)$HgBr_3$ (TMA = $(CH_3)_4N$) crystal [11] doped with Cu^{2+}, through the polarized optical absorption (OA) spectra. Attention is paid to correlate the absorption spectra with the local structure around Cu^{2+}. This crystal (monoclinic $P2_1$ space group) [12] is an attractive system for exploring new optical phenomena. In fact, the coordination geometry around the mercury cation (figure 1) is intermediate between the tetrahedral symmetry displayed by this cation in $(TMA)_2HgBr_4$ (orthorhombic $Pmcn$ space group) [13], and the trigonal symmetry (D_{3d}) displayed by Cd or Mn in (TMA)$CdBr_3$ and (TMA)$MnBr_3$ (hexagonal $P6_3/m$) [14, 15], whose MBr_6^{4-} units form infinite chains of face sharing octahedra. Furthermore, the crystal provides a low symmetry Hg^{2+} site for accommodating Cu^{2+}. Its ferroelectric properties seem to be associated with non-centrosymmetric distortions of the inorganic $[HgBr_3]_n^{n-}$ units rather than with the tetramethylammonium ions [12]. Interestingly, this work exploits the structural properties of a transparent anisotropic material like (TMA)$HgBr_3$ to find new optical phenomena using Cu^{2+} impurities as chromophore. Alternatively to pure copper compound research, this doping procedure extends the range of materials with potential applications as sensors.

(TMA)Hg[Cu]Br_3 is green at room temperature. This colour, which is different to those shown by other Cu^{2+}-doped bromide crystals containing either $CuBr_4^{2-}$ (purple) [9] or $CuBr_6^{4-}$ (red) [8] complexes, is due to the presence of an unusual $Br^- \rightarrow Cu^{2+}$ CT band at 15 800 cm^{-1}. This band appears shifted to lower energy with respect to the first CT transition in $CuBr_4^{2-}$ and $CuBr_6^{4-}$ (16 800 and 19 300 cm^{-1}, respectively). The band intensity exhibits different variations with temperature depending on the light polarization. The crystal shows a marked thermochromism below 100 K, and a strong dichroism at low temperature.

In this work, we report polarized CT spectra of (TMA)Hg[Cu]Br_3 and their dependence on temperature. The results are compared with those obtained in orthorhombic $(TMA)_2$Hg[Cu]Br_4 and $(TMA)_2$Cd[Cu]Br_4, and in hexagonal (TMA)Cd[Cu]Br_3 and (TMA)Mn[Cu]Br_3, where the Cu^{2+} coordination is $CuBr_4^{2-}$ (D_{2d} symmetry) [9] and $CuBr_6^{4-}$ (elongated D_{4h} symmetry) [8], respectively.

2. Experimental section

High optical-quality single crystals of (TMA)Hg[Cu]Br_3, (TMA)Mn[Cu]Br_3 and $(TMA)_2$Hg[Cu]Br_4 were grown by slow evaporation from solution at 40 °C. Suitable green ***b***-plates of (TMA)Hg[Cu]Br_3 were obtained from HBr (10%) acidic ethanol–water (1:1) solutions containing 1:2 and 1:3 stoichiometric ratios of (TMA)Br and $HgBr_2$ (or $MnBr_2$), respectively. The mercurate bromide concentration was intentionally duplicate or triplicate with respect to the expected 1:1 stoichiometry to avoid $(TMA)_2$Hg[Cu]Br_4 formation, favoured in highly acidic solutions [11]. 1–10 mol% of $CuBr_2$ was added to the solutions. Purple plates with rectangular or pseudohexagonal shapes of $(TMA)_2$Hg[Cu]Br_4 were grown from

solutions containing a 2:1 stoichiometric ratio of (TMA)Br and $HgBr_2$ using the previous solvent. Needle-like single crystals of (TMA)Mn[Cu]Br_3 were grown with the same procedure as employed for (TMA)Hg[Cu]Br_3. Crystal growing details for (TMA)Cd[Cu]Br_3 and $(TMA)_2$Cd[Cu]Br_4 are given elsewhere [8, 9]. The real Cu concentration in the crystal determined from atomic absorption spectroscopy is about 10% of the nominal Cu concentration.

The room temperature crystallographic structure of each compound was checked by x-ray diffraction using a Philips PW 1710 diffractometer. The x-ray diagrams of the investigated crystals were indexed according to structural data given in the literature. The lattice parameters obtained by fitting the observed Bragg peaks are the following: (TMA)Hg[Cu]Br_3 ($P2_1$ monoclinic space group; $a = 9.07(3)$ Å, $b = 15.95(5)$ Å, $c = 7.88(1)$ Å, $\beta = 93.65^\circ$) [12], $(TMA)_2$Hg[Cu]Br_4 ($Pmcn$ orthorhombic space group; $a = 9.31(2)$ Å, $b = 16.12(4)$ Å and $c = 12.78(2)$ Å) [13] and (TMA)Cd[Cu]Br_3 ($P6_3/m$ hexagonal space group; $a = 9.434(15)$ Å, $c = 7.034(3)$ Å) [14].

Several crystal plates for optical studies were selected and oriented with a polarizing microscope. The crystal plate orientation was checked by x-ray diffraction. The absorption spectra of single crystals were recorded with a Lambda 9 Perkin Elmer spectrophotometer equipped with Glan Taylor polarizing prisms and operating with a fixed bandwidth of 1 nm. Sample thicknesses for absorption were about 0.2–0.5 mm. The crystals were mounted on an OFHC copper plate over a 1 mm hole. A proper thermal contact was attained using crycon grease along two orthogonal crystal edges in order to minimize strains, and covered with a 1 mm drilled aluminium sheet as radiation shield. Crystals were oriented with the light polarization along the extinction directions, except for (TMA)Hg[Cu]Br_3, that was oriented along $\boldsymbol{a}$ due to domain formation, with a polarizing microscope. The temperature was varied in the 10–300 K range with a Scientific Instruments 202 closed-circuit cryostat and an APD-K controller providing a temperature accuracy of 1 K.

Specific heat measurements were carried out on the (TMA)Hg[Cu]Br_3 compound in the 2–300 K range in order to explore the existence of phase transitions below room temperature. The experiments were performed on a Physical Properties Measurement System (PPMS) from Quantum Design equipped with heat capacity option. The experimental $C_p(T)$ curve follows a typical Debye-type behaviour. Neither structural transition peak nor pretransitional effect associated with the ferroelectric phase transition is observed in the explored temperature range.

3. Results and discussion

3.1. Crystal structure

Figure 1 shows the unit cell of the (TMA)$HgBr_3$ crystal together with the coordination polyhedra around Hg. The structure can be regarded as built up from infinite chains of interconnected $HgBr_3^-$ units along the $\boldsymbol{c}$ direction [12]. The resulting Hg^{2+} polyhedra are either distorted corner-shared tetrahedra or face-shared octahedra depending on whether the Hg–Br bond length defining the coordination polyhedron is limited to 3.0 Å or to 5.5 Å, respectively. A regular hexahedral D_{3d} coordination for Hg, resembling the latter situation, would be expected for (TMA)$HgBr_3$ in the high-temperature paraelectric phase (TMMC-type structure) [11–13]. Due to the low symmetry of the Hg^{2+} site, the substitution of Hg^{2+} by Cu^{2+} in (TMA)$HgBr_3$ leads to a highly distorted local geometry beyond the usual Jahn–Teller distortion of D_{2d} ($CuBr_4^{2-}$) or D_{4h} ($CuBr_6^{4-}$) symmetry. This situation gives rise to new features in the CT spectra, not observed previously in Cu-doped systems containing either $CuBr_6^{4-}$ or $CuBr_4^{2-}$ [8, 9].

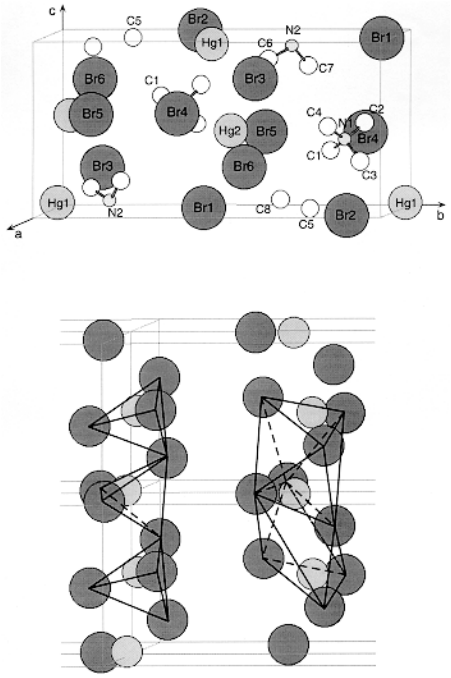

Figure 1. Crystallographic unit cell of (TMA)$HgBr_3$ (TMA = $(CH_3)_4N$) in the room-temperature monoclinic $P2_1$ ferroelectric phase. Lattice parameters: $a = 9.07$ Å, $b = 15.95$ Å, $c = 7.88$ Å, $\beta = 93.6^\circ$. Below, the cell is duplicated along the $\boldsymbol{a}$ and $\boldsymbol{c}$ monoclinic directions (The $\boldsymbol{a}$, $\boldsymbol{b}$ and $\boldsymbol{c}$ directions are the same in both figures). The Br coordination polyhedra around the mercury ions are shown (left) limiting the maximum Br–Hg bond distance to 3.0 Å and (right) to 5.5 Å. Note that the polyhedra form linear chains of corner-shared tetrahedra or face-shared octahedra along $\boldsymbol{c}$, respectively. The latter structure resembles the TMMC-type structure of the high-temperature isomorphous (TMA)(M)Br_3 (M = Mn, Cd) crystals [14, 15].

3.2. Polarized optical absorption spectroscopy

Figure 2 shows the OA spectra of (TMA)Hg[Cu]Br_3 with light polarized along the monoclinic $\boldsymbol{a}$ direction and perpendicular to $\boldsymbol{a}$ (nearly parallel to $\boldsymbol{c}$) at $T = 300$ and 10 K. A first account of these spectra was given elsewhere [16]. The $T = 300$ K spectra show two intense CT bands at 15 800 and 26 500 cm^{-1} which are similar to those observed in the optical spectra of the pure $[Cu(Ph_3AsO_4)][CuBr_4]$ crystal (olive green phase) [17]. The present work clarifies the ligand-to-metal CT origin of those bands, in particular, of the low lying band at 15 800 cm^{-1} whose intensity is two and one orders of magnitude higher than the corresponding CF (d–d) bands at 6400 and 7400 cm^{-1}, respectively (figure 3). These two near-IR bands are similar to those observed in JT distorted $CuBr_4^{2-}$ complexes (D_{2d}) [18]. According to the energy level diagram shown in the inset of figure 3, these bands are tentatively assigned to electronic transitions from the filled $e(xz, yz)$ and $a_1(z^2)$ orbitals to the half-filled $b_2(x^2 - y^2)$ orbital, respectively, since these are the only electric-dipole (ED) transitions allowed in D_{2d} symmetry. However, aside from the low symmetry ligand field of the Cu^{2+} complex, the intensity of these d–d bands is also activated by the vibronic mechanism, making difficult the analysis of the polarization behaviour of these nearly isotropic CF bands. The asymmetry displayed by the high energy band probably reflects the presence of the $b_1 \rightarrow b_2$ band partially allowed in the *actual* low-symmetry ligand-field in (TMA)Hg[Cu]Br_3 and by vibronic assistance.

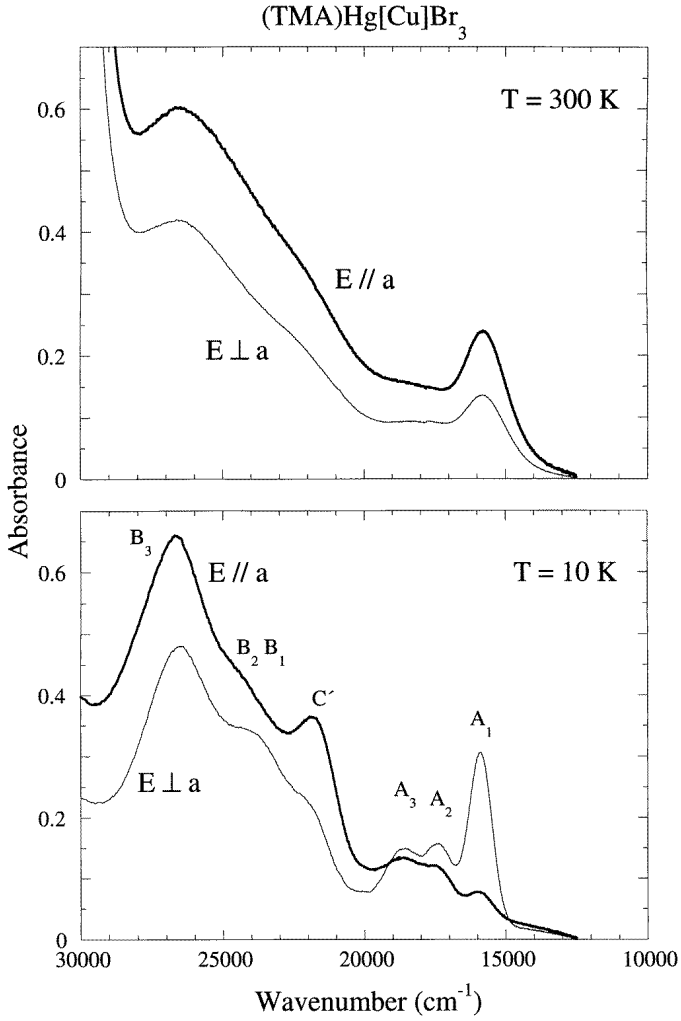

Figure 2. Polarized optical absorption spectra of the (TMA)Hg[Cu]Br_3 single crystal at $T = 300$ K and $T = 10$ K in the charge transfer region. Spectra were recorded with $\boldsymbol{E}$ parallel to $\boldsymbol{a}$ and perpendicular to $\boldsymbol{a}$ within the $\boldsymbol{b}$ plane. Sample thickness: 0.3 mm. The absorption bands are labelled according to the $CuBr_4^{2-}$ state diagram of figure 6.

CT bands appear resolved in the $T = 10$ K polarized spectra (figure 2). Three components, labelled A_1, A_2 and A_3, are observed in the first band at 15 800, 17 400 and 18 700 cm^{-1}, respectively, and three components at 21 800 (C′), 23 900 (B_1, B_2) and 26 700 cm^{-1} (B_3) are observed in the second band. Note that the first CT band responsible for the green colour, A_1, is strongly polarized at $T = 10$ K, whereas it shows an almost isotropic behaviour at room temperature. This explains the weak and strong dichroism observed with a polarizing microscope at room temperature and 10 K, respectively. The colour at low temperature is either green or garnet depending on whether the light electric field, $\boldsymbol{E}$, is directed along the monoclinic $\boldsymbol{a}$ direction or perpendicular to it in the $\boldsymbol{b}$ plane.

The relative intensity of the CT bands indicates that while bands at 15 800 (A_1) and 23 900 cm^{-1} (B_1) display a similar polarization behaviour with the distortion axis of the

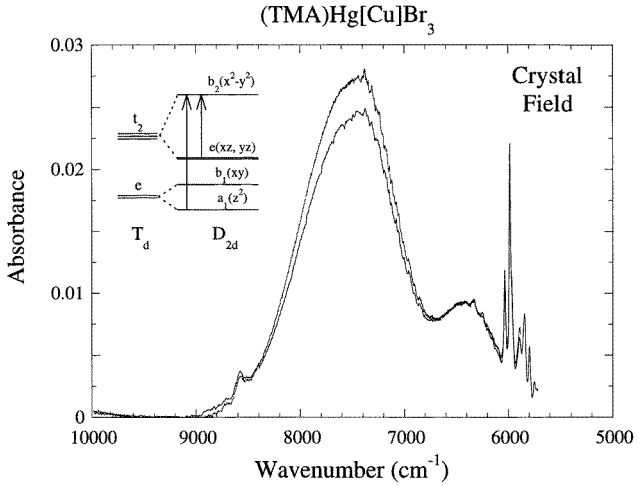

Figure 3. Polarized optical absorption spectra of the (TMA)Hg[Cu]Br_3 single crystal at $T = 10$ K in the near-IR crystal field region. Bands at 6400 and 7400 cm^{-1} correspond to d–d transitions of Cu^{2+}. The inset shows an schematic energy level diagram showing the electric-dipole allowed crystal-field transitions in d^9 for a D_{2d} symmetry $CuBr_4^{2-}$ complex. The sharp peak structures observed around 8600 and 6000 cm^{-1} are overtones of the tetramethylammonium ions. The absorbance scale is the same as used in figure 2.

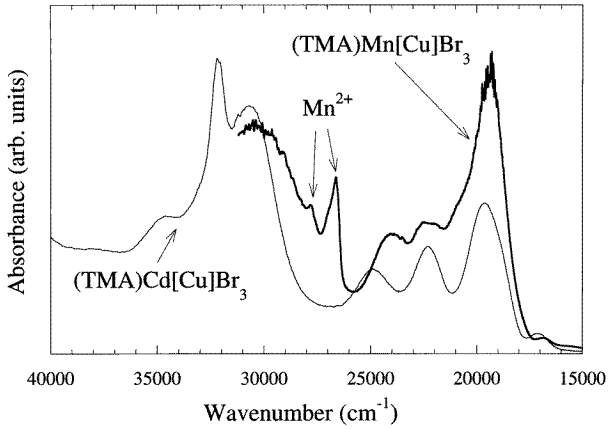

Figure 4. Polarized optical absorption spectra of the (TMA)Cd[Cu]Br_3 and (TMA)Mn[Cu]Br_3 crystals at $T = 10$ K with $\boldsymbol{E}$ perpendicular to the hexagonal $\boldsymbol{c}$ direction (i.e. perpendicular to the chain).

complex oriented near $\boldsymbol{c}$ (chain direction), bands at 17 400 (A_2), 187 00 (A_3), 21 800 cm^{-1} (C′), 245 00 (B_2) and 26 700 cm^{-1} (B_3) show a different polarization behaviour.

For comparison purposes, figures 4 and 5 show the OA spectra of (TMA)(M)[Cu]Br_3 (M = Cd, Mn) and $(TMA)_2$(M)[Cu]Br_4 (M = Cd, Hg). The spectra can be explained in terms of the $CuBr_6^{4-}$ (D_{4h}) and $CuBr_4^{2-}$ (D_{2d}) complexes, respectively [8, 9]. The comparison of these spectra with those of figure 2 indicates that the CT spectra of (TMA)Hg[Cu]Br_3 are somewhat in between those $CuBr_4^{2-}$ and $CuBr_6^{4-}$, but closer to $CuBr_4^{2-}$. The two groups of bands around 18 000 and 28 000 cm^{-1} observed in $(TMA)_2$(Cd, Hg)[Cu]Br_4 (figure 5) are

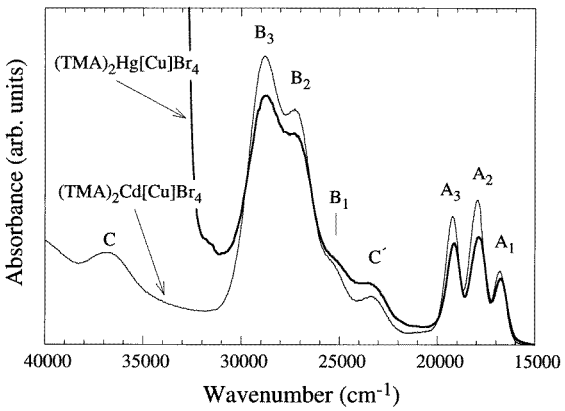

Figure 5. Polarized optical absorption spectra of $(TMA)_2Cd[Cu]Br_4$ and $(TMA)_2Hg[Cu]Br_4$ crystals at $T = 10$ K along the orthorhombic $\boldsymbol{b}$ direction. Bands are labelled according to the assignment given in figure 6 for a $CuBr_4^{2-}$ complex of D_{2d} symmetry [9, 18].

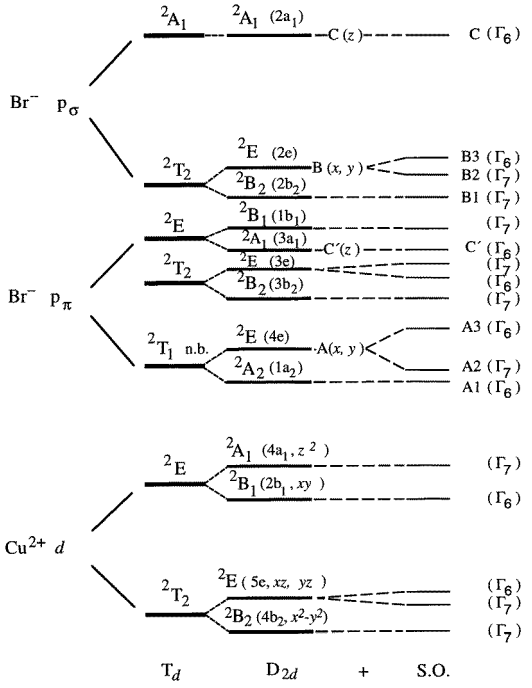

Figure 6. Approximate state diagram of a Jahn–Teller distorted $CuBr_4^{2-}$ complex of D_{2d} symmetry. The effect of the spin–orbit interaction of the Br ligands has been included. The electric-dipole transitions allowed in D_{2d} are $B_2 \rightarrow A_1$ (z polarized) and $B_2 \rightarrow E$ (x, y polarized). Transitions $\Gamma_7 \rightarrow \Gamma_7$ and $\Gamma_7 \rightarrow \Gamma_6$ are (x, y, z) and (x, y) polarized, respectively, when the spin–orbit interaction is considered. Some of the observed CT transitions are identified by the commonly used labels [9, 18].

assigned within a $CuBr_4^{2-}$ complex of D_{2d} symmetry [9, 18] to $Br^- \rightarrow Cu^{2+}$ CT transitions involving electronic jumps from the σ- and π-bonding mainly Br^- molecular orbitals (MOs)

of e and a_1 symmetry to the antibonding mainly Cu^{2+} $b_2(x^2 - y^2)$ MO (figure 6). In terms of electronic states, the $CuBr_4^{2-}$ bands A_1, A_2 and A_3 at 16 800, 17 900 and 19 200 cm^{-1} (figure 5) correspond to transitions from the $^2B_2$ ground state to the parent tetrahedral π-bonding $^2T_1$ CT state split into three components by ligand field distortions of D_{2d} symmetry, and the spin–orbit interaction of Br^- ligands ($2\Gamma_7 + \Gamma_6$ double group D_{2d} irreps) [18]. The CT band C′ at 23 500 cm^{-1} corresponds to the $^2A_1$ (Γ_6) state of the parent tetrahedral ^2E state, and the CT band with components B_1, B_2 and B_3 at 25 270, 27 250 and 28 800 cm^{-1} shows the highest intensity, and analogously corresponds to the three split components of the σ-bonding $^2T_2$ state. The CT bands of (TMA)Hg[Cu]Br_3 (figure 2) have been labelled as in figure 5 for $CuBr_4^{2-}$ taking into account the similitude of both spectra. Therefore the present analysis strongly suggest that Cu^{2+} enters the (TMA)Hg[Cu]Br_3 crystal as a substitutional impurity replacing Hg^{2+}. The redshift of 1200 cm^{-1} (A_1) and 500 cm^{-1} (A_2 and A_3) shown by the first CT band on passing from $(TMA)_2$Hg[Cu]Br_4 to (TMA)Hg[Cu]Br_3 must be associated with higher distortions of the $CuBr_4^{2-}$ complex in the ferroelectric crystal according to expectations on the basis of the Hg^{2+} local structure (figure 1) [12]. The strong polarization shown by A_1 in comparison to the other CT bands observed in the OA spectrum is noteworthy. This behaviour contrasts with the similar nearly isotropic polarization exhibited by A_1, A_2 and A_3 in the undistorted D_{2d} $CuBr_4^{2-}$ complex in $(TMA)_2$Hg[Cu]Br_4 (figure 5). The polarization of A_1 in the thermochromic (TMA)Hg[Cu]Br_3 crystal is probably associated with the lengthening of one Cu–Br bond along the chain ($\boldsymbol{c}$ direction) imposed by crystal anisotropy. Such distortion must give rise to a $Br^- \rightarrow Cu^{2+}$ CT transition strongly polarized along the elongated Cu–Br bond, with an energy shifted to lower energies in comparison to the undistorted D_{2d} $CuBr_4^{2-}$ complex formed in $(TMA)_2$Hg[Cu]Br_4. This interpretation is supported by the A_1 redshift of 1200 cm^{-1} observed on passing from $(TMA)_2$Hg[Cu]Br_4 to (TMA)Hg[Cu]Br_3. Note that this redshift is not observed in $CuBr_4^{2-}$ along the $(TMA)_2$(M)[Cu]Br_4 series M = Mn → Cd → Hg (figure 5 and [9]). In contrast to (TMA)Hg[Cu]Br_3, the MBr_4^{2-} complexes are independent units in $(TMA)_2MBr_4$ and, therefore, the formed $CuBr_4^{2-}$ impurities can adopt a similar coordination geometry independent of M, making the first CT band insensitive to chemical pressure effects [19].

4. Variation of the CT spectra with temperature

Figure 7 depicts the variation of the integrated band area, $A(T)$, corresponding to the first CT band (A_1) of (TMA)Hg[Cu]Br_3 with $\boldsymbol{E}$ along $\boldsymbol{a}$ and in the perpendicular direction within the ac plane. The observed variation of $A(T)$ reflects the progressive enhancement of dichroism upon decreasing temperature below 100 K and is repetitive for different heating–cooling runs. This thermal-induced dichroism is also accompanied by a change of colour (thermochromism) when the crystal is observed with polarized light along $\boldsymbol{a}$. The analysis of these variations suggests that the change of the polarized intensity with temperature is presumably related to thermally activated reorientations of the highly distorted $CuBr_4^{2-}$ units, rather than to continuous rotations of the complex induced by temperature. The latter effect is unlikely to be due to constraints imposed by crystal anisotropy. The possibility of structural distortions of the complex, as responsible for the observed temperature variations, must be ruled out. In fact, neither the CT energy nor the band structure, strongly dependent on structural distortions, changes in the 10–300 K temperature range. In addition, we have detected no evidence of phase transition in (TMA)$HgBr_3$ between 2 and 300 K from specific heat measurements shown in figure 8(a). Finally, exchange effects between Cu^{2+} ions, analogous to those proposed in $KCuCl_3$ or in $LiCuCl_3.2H_2O$ [20] to explain the strong temperature variation of intensity, must be also ruled out in the present compound given that we are dealing with *diluted systems*. Moreover, the

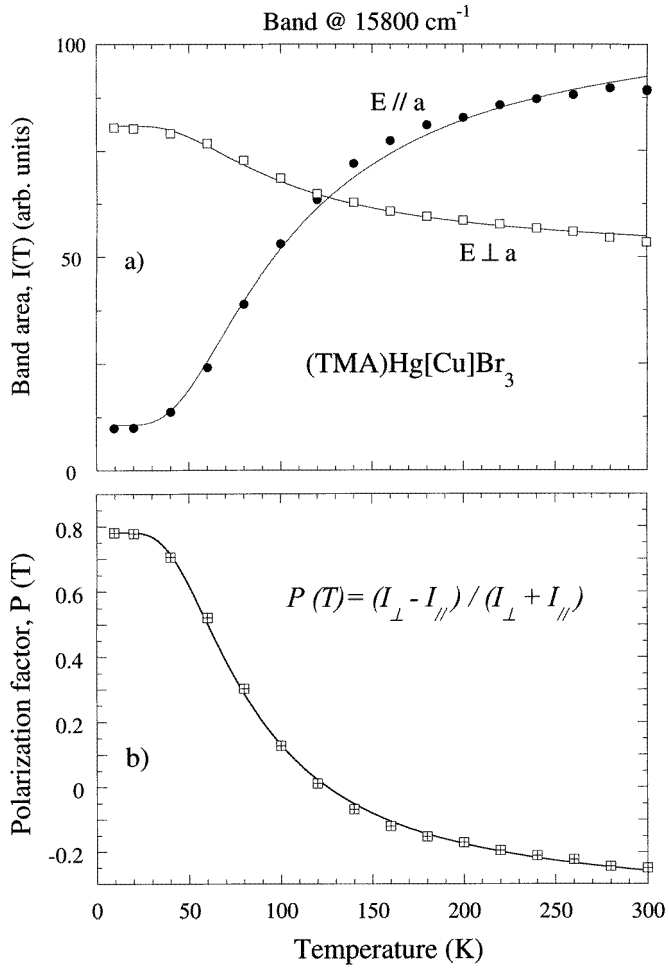

Figure 7. Temperature dependence of (a) the integrated intensity, $I(T)$, of the A_1 band at 15 800 cm^{-1} along $\boldsymbol{a}$ and perpendicular to $\boldsymbol{a}$ and (b) the polarization factor, $P(T)$. Lines in (a) represent the least-squares fitting of the experimental $I_i(T)$ data to equation (1). The superscripts 1 and 2 denote polarization with $\boldsymbol{E}$ parallel and perpendicular to $\boldsymbol{a}$, respectively. The fit parameters are $I_1^{gr} = 10$, $I_1^{ex} = 430$, $I_2^{gr} = 80$, $I_2^{ex} = 115$ (relative units) and $\Delta E = 130$ cm^{-1}. The curve in (b) is the fit of data $P(T)$ to equation (2) with $a = 0.78$, $b = 4.6$, $d = 6.2$ and $\Delta E = 130$ cm^{-1}.

OA spectrum does not depend on the Cu concentration in the investigated 1–0.1 mol% range. Preliminary EPR measurements support this view. Actually, $A(T)$ can be explained in terms of orientational hopping of the Cu^{2+} complexes among four potential wells associated with each possible Cu–Br elongation. A similar model based on three non-equivalent potential wells related to the different distortions of a $CuBr_6^{4-}$ complex in a pseudo-trigonal site was proposed elsewhere [16]. At low temperature, only the minimum energy configuration is populated and, according to spectra of figure 2, it must correspond to the $CuBr_4^{2-}$ orientation having the Cu–Br distortion near along $\boldsymbol{c}$ on the ac plane. Upon increasing temperature, orientations associated with higher energy potential wells become populated, thus leading to a reduction of dichroism.

In order to justify the proposed model, note that there are four equivalent configurations

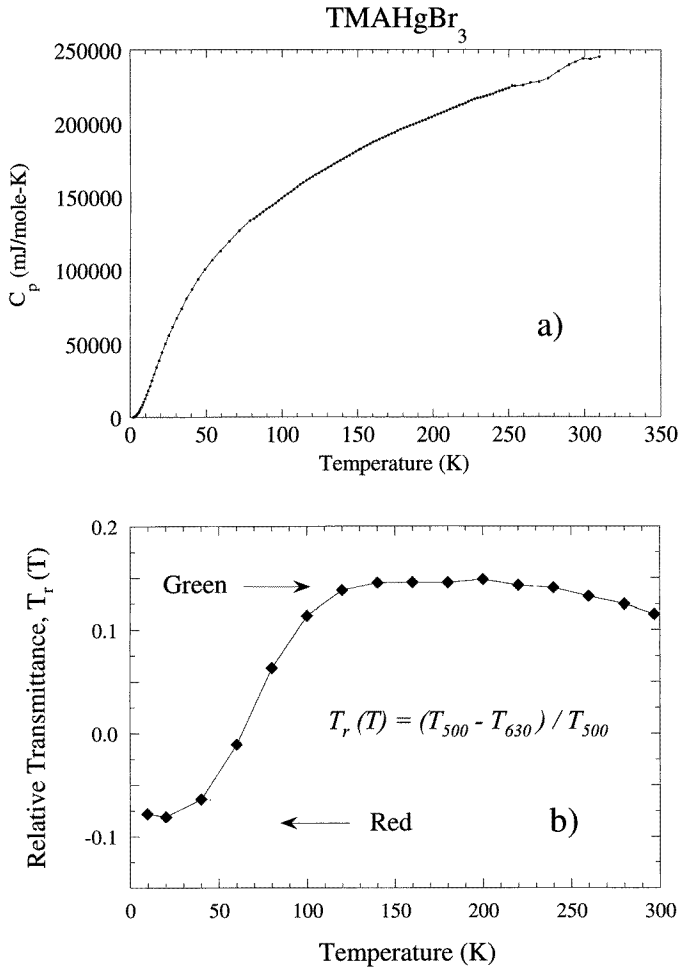

Figure 8. Temperature dependence of (a) the specific heat, $C_p(T)$, of (TMA)Hg[Cu]Br_3 in the 2–300 K range, and (b) the relative transmittance, $T_r(T)$, in $\boldsymbol{a}$ polarization. The T_r parameter indicates the relevant crystal colour between the two extreme values: $T_r = 0.15$ (green) and $T_r = -0.1$ (red). Thermochromism is revealed by the strong variation of T_r between 50 and 100 K.

related to the elongated Cu–Br bond in a tetrahedral $CuBr_4^{2-}$ complex. However, this orientational degeneracy is lifted in (TMA)$HgBr_3$ by crystal anisotropy and, therefore, preferential orientations are expected for $CuBr_4^{2-}$ in this crystal. In fact, the Cu–Br distortion along the chain direction is greatly favoured with respect to the other three orientations in the (TMA)Hg[Cu]Br_3 host crystal (figure 1). The intensity variations of figure 7 can be accounted for within this model taking into account that the minimum energy configuration for $CuBr_4^{2-}$ at low temperature corresponds to that orientation with the Cu–Br elongation near along $\boldsymbol{c}$. Upon increasing temperature, the other three configurations are thermally populated, thus leading to a change of the polarized spectrum. Thus this explains why the maximum A_1 intensity is observed along $\boldsymbol{c}$ (figures 3 and 7). On the assumption that there is one stable complex and three degenerated excited configurations with an effective mean energy separation ΔE, then the integrated polarized intensity, $I_i(T)$, of the A_1 CT band along the i polarization as a

function of temperature is given by

$$I_i(T) = \frac{I_i^{gr} + I_i^{ex}\exp(-\Delta E/kT)}{1 + 3\exp(-\Delta E/kT)}. \quad (1)$$

I_i^{gr} and I_i^{ex} represent the i-polarized absorption intensity for the stable complex configuration (gr) and the three excited configurations (ex), respectively. The curves of figure 7(a) have been calculated within this model by fitting the experimental $I_i(T)$ values to equation (1). The fit parameters are $I_1^{gr} = 10$ and $I_1^{ex} = 430$ for $\boldsymbol{E}$ parallel to $\boldsymbol{a}$, and $I_2^{gr} = 80$ and $I_2^{ex} = 115$ for $\boldsymbol{E}$ perpendicular to $\boldsymbol{a}$. The activation energy, ΔE, was firstly determined through the analysis of the temperature dependence of the polarization factor defined as $P(T) = [I_2 - I_1]/[I_2 + I_1]$. The use of $P(T)$ is advantageous since it provides precise information on the thermal behaviour of the CT band in order to obtain suitable values of ΔE. In fact, $P(T)$ does not depend on the possible change of the CT oscillator strength with temperature but on their relative values. Figure 7(b) depicts the polarization factor $P(T)$ as a function of temperature. This parameter illustrates the degree of dichroism of the crystal. The solid curve was obtained by fitting data to

$$P(T) = \frac{a[1 - b\exp(-\Delta E/kT)]}{1 + d\exp(-\Delta E/kT)}. \quad (2)$$

These parameters are related to equation (1) by $a = (I_2^{gr} - I_1^{gr})/(I_2^{gr} + I_1^{gr})$; $b = (I_1^{ex} - I_2^{ex})/(I_2^{gr} - I_1^{gr})$; $d = (I_2^{ex} + I_1^{ex})/(I_2^{gr} + I_1^{gr})$. The fit values are $a = 0.78$, $b = 4.6$, $d = 6.2$ and $\Delta E = 130\ cm^{-1}$.

Note that the strongest dichroism exhibited by this crystal at $T = 10$ K corresponds to the highest value $P = 0.78$. The progressive loss of dichroism upon heating is reflected by the decrease of $P(T)$ tending to a constant value of $P = -0.38$ in the high temperature limit. Within the proposed model, the decrease of $P(T)$ is related to the orientational disorder associated with the thermal activation of different excited configurations of the copper complex.

5. Thermochromism

An useful parameter for exploring the thermochromic properties of the present crystal is the relative transmittance, T_r, which relates the difference between the transmitted light at 500 nm (green) and 630 nm (red): $T_r = [T_{500} - T_{630}]/T_{500}$. These wavelengths correspond to the maximum crystal transmittance in the visible range and the absorption maximum of the A_1 CT band, respectively. The parameter is normalized to the 500 nm transmittance. As shown in figure 8(b), the variation of $T_r(T)$ indicates that the change of colour takes place between 50 and 100 K. Interestingly, the thermochromism is not related to any phase transition of the host (TMA)$HgBr_3$ crystal as is shown in the specific heat curve of figure 8(a), but it varies continuously over a wide temperature range, supporting the existence of thermal activated processes in the Cu^{2+} chromophores.

6. Conclusions

We have formed a new thermochromic material, (TMA)Hg[Cu]Br_3, on the basis of the low symmetry structure of the host crystal and the properties of the JT $CuBr_4^{2-}$ complexes as chromophore. In addition to the thermochromism, the crystal exhibits a temperature-induced dichroism that is associated with non-equivalent orientations of the copper complexes. Both the green to red change of colour and the dichroism are explained in terms of intensity variations of the low energy $Br^- \rightarrow Cu^{2+}$ CT band at 15 800 cm^{-1}. The presence of this intense CT band is noteworthy since it has never been observed in the optical spectra of *isolated* $CuBr_4^{2-}$ complexes

of D_{2d} symmetry. Its origin seems to be related to additional low-symmetry distortions of the copper complex due to the crystal anisotropy of (TMA)$HgBr_3$. This conclusion is supported by the comparative analysis carried out between the CT spectra of the present (TMA)Hg[Cu]Br_3 crystal and other similar Cu^{2+}-doped bromides containing $CuBr_4^{2-}$ and $CuBr_6^{4-}$ of D_{2d} and D_{4h} symmetry, respectively.

Acknowledgments

We thank S Sharif, Erasmus student from the University of Leicester for his kindly collaboration in this work. The authors are indebted to Professor L Lezama (University of Pais Vasco) for EPR facility and technical assistance. Also fruitful discussions with Professor L Lezama, Professor M Moreno (University of Cantabria) and Professor M Hitchman (University of Tasmania) are acknowledged. We thank the group of Professor J C Gómez-Sal (University of Cantabria) for doing the first calorimetric measurements of the title compound. This work was supported by Caja Cantabria and the CICYT (project No PB95-0581).

References

[1] Lever A B P 1984 *Inorganic Electronic Spectroscopy* (New York: Elsevier)
[2] Willett R D, Haugen J A, Lebsack J and Morrey J 1974 *Inorg. Chem.* **13** 2510
[3] Hathaway B J 1984 *Struct. Bonding* **57** 55
[4] Hitchman M A 1994 *Comments Inorg. Chem.* **15** 197
[5] Valiente R and Rodríguez F 1996 *J. Phys. Chem. Solids* **57** 571
[6] Bloomquist D R, Pressprich M R and Willett R D 1988 *J. Am. Chem. Soc.* **110** 7391
[7] Willett R D 1964 *J. Chem. Phys.* **41** 2243
[8] Valiente R, Marco de Lucas M C and Rodríguez F 1994 *J. Phys.: Condens. Matter* **6** 4527
[9] Valiente R, Marco de Lucas M C and Rodríguez F 1995 *J. Phys.: Condens. Matter* **7** 3881
[10] Jørgensen C K 1970 *Prog. Inorg. Chem.* **12** 101
[11] Fatuzzo E, Nitsche R, Roetschi H and Zingg S 1962 *Phys. Rev.* **125** 514
[12] White J G 1962 *Acta Crystallogr.* **16** 397
[13] Kamenar B and Nagl A 1976 *Acta Crystallogr.* **32** 1414
[14] Asahi T, Hasebe K and Gesi K 1990 *Acta Crystallogr.* C **46** 2252
[15] Alcock N W and Holt S L 1978 *Acta Crystallogr.* B **34** 1970
[16] Valiente R and Rodríguez F 1997 *Z. Phys. Chem.* **201** 159
[17] Massabni A C, Nascimento O R, Halvorson K and Willett R D 1992 *Inorg. Chem.* **31** 1779
[18] Marco de Lucas M C and Rodríguez F 1993 *J. Phys.: Condens. Matter* **5** 2625
[19] Valiente R and Rodríguez F 1998 *J. Phys.: Condens. Matter* **10** 9525
[20] Desjardins S R, Wilcox D E, Musselman R L and Solomon E I 1987 *Inorg. Chem.* **26** 288